Line-of-Sight Vector Adjustment Model for Geopositioning of SPOT-5 Stereo Images

Hyung-Sup Jung, Sang-Wan Kim, Joong-Sun Won, and Dong-Cheon Lee

Abstract

We formulate and present a new geopositioning method for SPOT-5 High-Resolution Geometric (HRG) stereo images, named the line-of-sight (LOS) vector adjustment model. It is applicable to satellites that move along a well-defined close-to-circular elliptical orbit with a predicted orbit close to true. SPOT-5 satisfies these requirements because it has the improved capability of providing accurate satellite attitude and a look angle for each detector. The method's core idea is that only the LOS vector was adjusted when correcting the geometric distortion of SPOT-5 imagery. One advantage of this method is that it achieves high geopositioning accuracy with a limited number of ground control points (GCPs). Although a minimum of three GCPs is needed for processing, a test result satisfied the accuracy requirement within one pixel of a SPOT-5 panchromatic image even with only three GCPs. The performance in terms of root mean square error (RMSE) improved as the number of GCPs increased. Five GCPs were found to be the optimal number in the practical application of the LOS vector adjustment model. Using five GCPs, the RMSEs were 0.48 m and 0.64 m in planimetry and height, respectively. The test results indicate that the proposed method is superior to the bundle adjustment method for the geopositioning of SPOT-5 HRG stereo images.

Introduction

Since SPOT-1 was launched in 1986, the SPOT satellites have acquired a large number of stereo pairs. These have been used for urban and regional mapping, disaster management, classification, and many other purposes (Gugan and Dowman, 1988; Yesou and Rolet, 1990; Baraldi and Parmiggiani, 1990). The SPOT systems have, however, the constraints of mis-registration caused by errors in the initial parameters and a low spatial resolution. SPOT-5 is mounted with two High-Resolution Geometric (HRG) viewing instruments that have resolutions of 5 m in the panchromatic and 10 m in the multispectral modes; it also has an improved capability of location accuracy by using a geometrically optimized system (Bouillon *et al.*, 2003; Nonin and Piccard, 2003).

Many researchers have previously investigated the geometry of SPOT imagery. The geometric characteristics have been well-studied, and various mathematical models have been proposed. These models can be divided into three main categories based on their different functions and parameters: the bundle adjustment method is based on extended collinearity equations; a further model involves direct linear transformation (DLT); and an orbital resection model utilizes orbital elements rather than the position and velocity of a satellite.

Bundle adjustment (Orun and Natarajan, 1994; Mahapatra *et al.*, 2004) is a traditional method based on the collinearity condition, which states that the exposure station, and any ground and image points, all lie along a straight line. The position and attitude of the satellite are used for the model parameters, and are represented by second-order polynomials of time. The optimal local orbit and attitude are calculated by using ground control points (GCPs) with extended collinearity equations; the accuracy of geometric correction obtained is relatively good. For these reasons, this is the most popular method used for the registration of SPOT imagery (Chen and Rau, 1993; Buyuksalih *et al.*, 2005), but it has a disadvantage in that more than six GCPs are generally required.

The DLT method (Gupta and Hartley, 1997) is derived from two simplifying assumptions that the sensor array is traveling in a straight line, and its orientation is constant over the image acquisition duration. Under these assumptions, the camera model is represented by a nonlinear Cremona transformation of object space into image space. This method has advantages in the geometric correction of satellite images without orbit information and in computational efficiency. However, more than six GCPs are required for this method also, and the accuracy of geometric correction using DLT is relatively poor.

The orbital resection model (Salamonowicz, 1986; Gugan and Dowman, 1988; Radhadevi *et al.*, 1994; Zoej and Petrie, 1998) is based on the general assumption that the satellite has an approximate Keplerian trajectory (Kratky, 1989) in which the position and attitude of a sensor vary continually in a systematic way to keep the satellite pointing towards the center of the Earth. This model is represented by an orthogonal rotation matrix to transform from the geocentric to the sensor coordinate system using the orbit attitude and four orbit parameters. Generally, two orbit parameters of the four are used for the model parameters. This method requires fewer GCPs than the others, and the resulting precision largely depends on the accuracy of the initial orbit parameters used. However, it is difficult to utilize all the

Hyung-Sup Jung and Joong-Sun Won are with the Department of Earth System Sciences, Yonsei University, 134 Sinchon-Dong, Seodaemun-Gu, Seoul 120–749, Korea (geohyung@yonsei.ac.kr; jswon@yonsei.ac.kr).

Sang-Wan Kim and Dong-Cheon Lee are with the Department of Geoinformation Engineering, Sejong University, 98 Gunja-Dong, Gwangjin-Gu, Seoul 143–747, Korea (swkim@sejong.ac.kr; dclee@sejong.ac.kr).

Photogrammetric Engineering & Remote Sensing
Vol. 73, No. 11, November 2007, pp. 1267–1276.

0099-1112/07/7311–1267/$3.00/0

parameters provided as auxiliary data, and it is not easy to correct geometric distortion.

In this paper, a new geometric correction method is proposed that is specifically designed to suit SPOT-5 imagery. The proposed approach is aimed at full exploitation of the improved capabilities in SPOT-5, which are the corrected attitude values and a look angle for each detector that accommodates the distortion of the lens. The new method, named the line-of-sight (LOS) vector adjustment model, is similar to the orbital resection model in that four orbit parameters are involved. It differs, however, from previous methods in that a main adjusting model parameter for the new method is the LOS vector only. Two equations are derived from the satellite geometry for SPOT-5 geometric correction, and two assumptions are required:

1. The satellite is moving along a well-defined close-to-circular elliptical orbit.
2. The predicted orbit recorded in the auxiliary data is close to the true satellite orbit.

The LOS vector adjustment model uses all the parameters available in the auxiliary data such as attitude angles, ephemeris points, look angles, and other factors. It also performs a restitution of satellite imagery using additional correction terms, which adjusts the LOS vector as a function of image lines and pixels for exterior orientation.

Mathematical formulae for the new model are derived in the next section. The proposed method was tested by using a SPOT-5 stereopair. The results are discussed with regard to the accuracy assessed with different numbers and distributions of GCPs. The effectiveness of the proposed method is compared with that of the bundle adjustment approach.

Mathematical Model

Satellite Geometry

A polar orbital satellite usually moves along a well-defined, close-to-circular elliptical orbit. Figure 1 illustrates the relationship between the satellite position in an orbit and its ground position on Earth. Position vector $\overrightarrow{P}$ is a vector from the Earth's center to a point P given on the Earth's surface, $\overrightarrow{u}$ is a LOS vector, and the satellite position vector $\overrightarrow{s}$ is a vector from the Earth's center O to the satellite position S. These vectors satisfy the following equation:

$$\overrightarrow{p} - \overrightarrow{s} = \mu \overrightarrow{u} \tag{1}$$

where μ is an arbitrary factor.

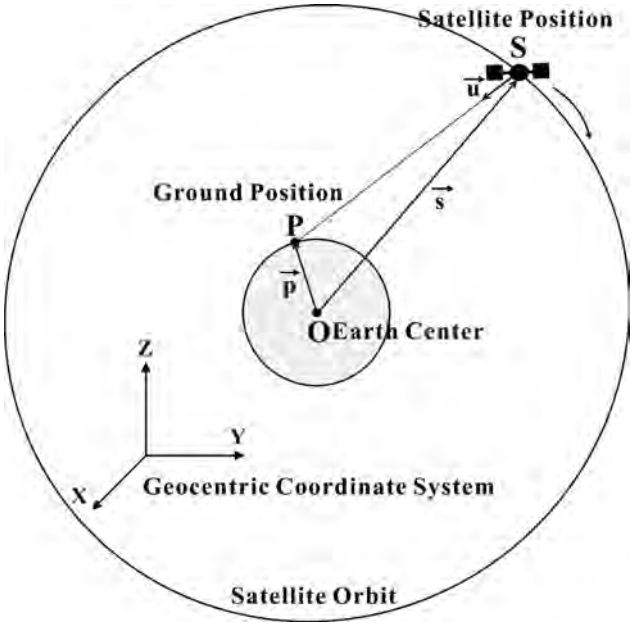

Figure 1. The relationship between ground and satellite positions.

Reference Systems

Coordinate systems needs to be defined to formulate a mathematical model for satellite geometry, and we follow the general convention.

The Earth-centered inertial (ECI) coordinate system has its origin at the mass center of the Earth with a fixed inertial direction along the intersection of the Earth's equatorial. The ecliptic planes and satellite positions are referred to it.

The Earth-centered Earth-fixed (ECEF) coordinate system measures ground position. The origin locates at the mass center of the Earth but is fixed in the Earth with its axis through the Greenwich meridian (or zero longitude).

A local orbital (LO) coordinate system has its origin at the mass center of the satellite. It moves with respect to time. Z is the same direction as the satellite position vector, X is the direction of the satellite velocity vector, and Y forms a right-handed reference coordinate normal to X and Z.

An attitude measurement (AM) coordinate system is fixed in relation to the satellite body. It is identical to the LO coordinate system when the satellite attitude angles are all zero. However, the satellite attitude angles are in reality rarely zero.

The image coordinate system is given by a pixel (j) and line (i) position.

Definition of Rotation Matrices

To formulate a mathematical model, two orthogonal rotation matrices must be defined. One matrix is an AM–LO rotation matrix M_A, and the other is a LO–ECI rotation matrix M_E. The AM–LO rotation matrix M_A is used to transform an AM coordinate system into a LO system. It accounts for the rotation of attitude angles, which vary with time. It is defined by the roll angle (ω), the pitch angle (φ), and the yaw angle (κ). These attitude angles can be approximated (Orun and Natarajan, 1994; Zoej and Petrie, 1998) by second-order polynomials such as the following:

$$\omega(t) = \omega_0 + \omega_1 \cdot t + \omega_2 \cdot t^2, \tag{2}$$

$$\varphi(t) = \varphi_0 + \varphi_1 \cdot t + \varphi_2 \cdot t^2, \text{ and} \tag{3}$$

$$\kappa(t) = \kappa_0 + \kappa_1 \cdot t + \kappa_2 \cdot t^2, \tag{4}$$

Westin (1990) chose to use bilinear, bicubic, or spline interpolation on roll, pitch, and yaw angles. These attitude angles are generally represented by a sinusoidal function of time. If the change in the amplitude of sinusoidal function is too small, second-order polynomials can be used. Alternatively, if the attitude information is relatively accurate and the variation of attitude angles is relatively high, the interpolation method is effective. In this study, a cubic spline interpolation method was applied to attitude information, because the SPOT-5 HRG image has high-resolution and corrected attitude angles.

The LO–ECI rotation matrix M_E transforms the LO coordinates into an ECI system. It assumes that the satellite trajectory is approximately Keplerian, and that the Earth is spherical and gravitational force is directed towards the Earth's mass center. This trajectory is characterized by a set of six orbital parameters, which are: half major axis (a), eccentricity

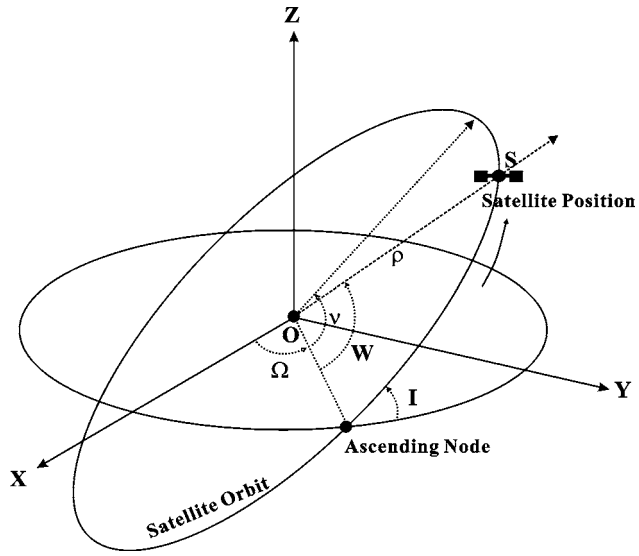

Figure 2. Satellite orbit parameters: longitude of ascending node (Ω), inclination of orbit plane (I), latitude argument of the satellite (W), and latitude argument of the perigee (υ).

(e), longitude of the ascending node (Ω), inclination of the orbit plane (I), latitude argument of the perigee (ν), and the latitude argument of the satellite (W). Figure 2 shows the orbital parameters and the related geometry. Using these parameters, the matrix M_E is defined as an orthogonal matrix.

These orbital parameters are calculated by the satellite position vector ($\overrightarrow{S}$) and the velocity vector ($\overrightarrow{V}$) (Slama *et al.*, 1980) as follows:

$$\overrightarrow{C} = \overrightarrow{S} \times \overrightarrow{V} = \begin{bmatrix} C_x \\ C_y \\ C_z \end{bmatrix}, \tag{5}$$

$$C = \left\| \overrightarrow{C} \right\|, \tag{6}$$

$$\rho = \left\| \overrightarrow{S} \right\|, \tag{7}$$

$$\cos I = \frac{C_z}{C}, \tag{8}$$

$$\tan \Omega = \frac{C_x}{C_y}, \text{ and} \tag{9}$$

$$\sin W = \frac{z}{\rho \cdot \sin I}, \tag{10}$$

where $\overrightarrow{C}$ is a vector normal to the orbital plane, and ρ is the distance between the Earth's center and the satellite. The parameters of I, Ω, W, and ρ are expressed as functions of time given as follows (Radhadevi *et al.*, 1998):

$$\Omega(t) = \Omega_0 + \Omega_1 \cdot t, \tag{11}$$

$$I(t) = I_0 + I_1 \cdot t, \tag{12}$$

$$W(t) = W_0 + W_1 \cdot t + W_2 \cdot t^2 + W_3 \cdot t^3, \text{ and} \tag{13}$$

$$\rho(t) = \rho_0 + \rho_1 \cdot t + \rho_2 \cdot t^2 + \rho_3 \cdot t^3 \tag{14}$$

For the parameter W, Radhadevi *et al.* (1998) proposed the first order polynomials. However, the regression analysis of W in this study revealed that the third order polynomials performed better than the first order polynomials as in the Equation 13.

LOS Vector Adjustment Model

The proposed LOS vector adjustment model is based on the assumptions that the satellite is moving along a well-defined close-to-circular elliptical orbit and that the predicted orbit recorded in auxiliary data is close to the true orbit. Figure 3 displays the geometry of true and adjusted LOS vectors. The predicted position of the satellite given by auxiliary data differs from the true position as shown in Figure 3. The geometry of the image can be corrected by adjusting the LOS vector, provided that the above assumptions are satisfied.

Here we formulate two equations for geopositioning of SPOT-5 image and introduce the LOS vector adjustment model as functions of the look angle. These are directly derived from the geometry shown in Figure 1. The position and LOS vectors of Equation 1 are transformed into a LO coordinate system using the rotation matrices of M_A and M_E, and thus Equation 1 in the LO coordinate system can be reformulated, as given by:

$$M_E^T \cdot \begin{bmatrix} p_x \\ p_y \\ p_z \end{bmatrix} - \begin{bmatrix} 0 \\ 0 \\ \rho \end{bmatrix} = \mu \cdot M_A \cdot \begin{bmatrix} u_x \\ u_y \\ u_z \end{bmatrix} \tag{15}$$

where (p_x, p_y, p_z) and (u_x, u_y, u_z) are the elements of vectors $\overrightarrow{p}$ and $\overrightarrow{u}$, respectively. The inverse of M_E is equal to the transpose of M_E. If the transpose of a rotational matrix M_A is multiplied on both sides, equation (15) is given as follows:

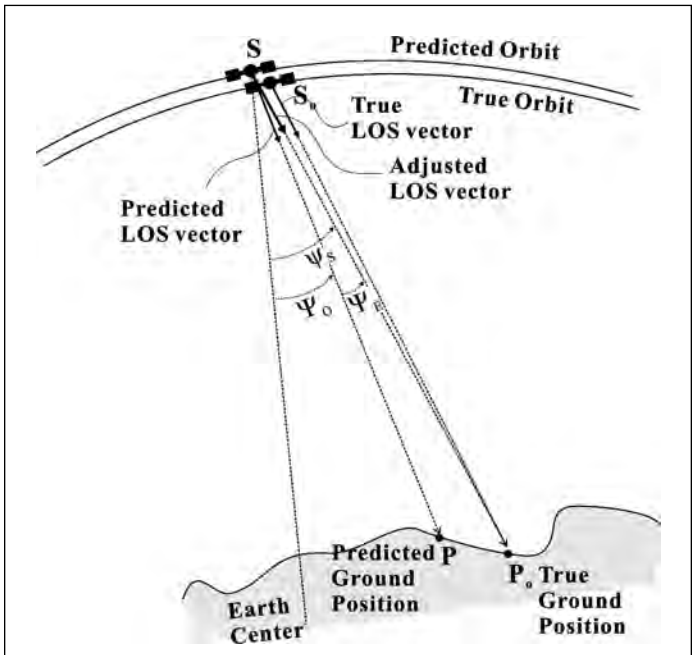

Figure 3. Geometry of the restitution of satellite imagery and LOS vectors.

$$M_A^T \cdot M_E^T \cdot \begin{bmatrix} p_x \\ p_y \\ p_z \end{bmatrix} - M_A^T \cdot \begin{bmatrix} 0 \\ 0 \\ \rho \end{bmatrix} = \mu \cdot \begin{bmatrix} u_x \\ u_y \\ u_z \end{bmatrix}. \quad (16)$$

To simplify Equation 16, two matrices of M_B and M_R are introduced as follows:

$$M_R \cdot \begin{bmatrix} p_x \\ p_y \\ p_z \end{bmatrix} - M_B \cdot \begin{bmatrix} 0 \\ 0 \\ \rho \end{bmatrix} = \mu \cdot \begin{bmatrix} u_x \\ u_y \\ u_z \end{bmatrix}. \quad (17)$$

If the arbitrary factor μ is eliminated in Equation 17, the equation is expressed by the following two equations:

$$\frac{r_{11}p_x + r_{12}p_y + r_{13}p_z - b_{13}\rho}{r_{31}p_x + r_{32}p_y + r_{33}p_z - b_{33}\rho} = \frac{u_x}{u_z}, \text{ and} \quad (18)$$

$$\frac{r_{21}p_x + r_{22}p_y + r_{23}p_z - b_{23}\rho}{r_{31}p_x + r_{32}p_y + r_{33}p_z - b_{33}\rho} = \frac{u_y}{u_z}, \quad (19)$$

The elements of the LOS vector (u_x, u_y, u_z) are functions of the look angle:

$$u_x = \tan(\psi_{ox}), \quad (20)$$

$$u_y = \tan(\psi_{oy}), \text{ and} \quad (21)$$

$$u_z = -1, \quad (22)$$

where ψ_{Ox} and ψ_{Oy} are look angles in the X and Y directions in the AM coordinate system.

Using Equations 20, 21, and 22, Equations 18 and 19 can be set out as:

$$f_1 \equiv \tan^{-1}\left[\frac{r_{11}p_x + r_{12}p_y + r_{13}p_z - b_{13}\rho}{r_{31}p_x + r_{32}p_y + r_{33}p_z - b_{33}\rho}\right] \quad (23)$$

$$+ \psi_{Ox} = -\psi_{Sx} + \psi_{Ox} = 0, \text{ and}$$

$$f_2 \equiv \tan^{-1}\left[\frac{r_{21}p_x + r_{22}p_y + r_{23}p_z - b_{23}\rho}{r_{31}p_x + r_{32}p_y + r_{33}p_z - b_{33}\rho}\right] \quad (24)$$

$$+ \psi_{Oy} = -\psi_{Sy} + \psi_{Oy} = 0,$$

where f_1 and f_2 are residuals, and ψ_{Sx} and ψ_{Sy} are look angles defined by the vector between the ground and satellite positions (see Figure 3).

If the orbital parameters such as satellite attitude, ephemeris points, and look angles are ideally exact, the equations will amount to zero. However, the f_1 and f_2 in Equations 23 and 24 are not zero in reality because of the uncertainty of the orbital parameters. There are normally non-zero residuals when they are calculated using the predicted orbit. These residuals are caused by error in look angles, and can be removed by changing the look angle. In consequence, the distortion in geometry can be corrected by adjusting the LOS vector, which is a function of the look angle (Jung *et al.*, 2004). Residuals can be removed by adding error look angles (ψ_E) as follows.

$$f_1(i,j) + \psi_{Ex}(i,j) = -\psi_{sx}(i) + \psi_{ox}(j) + \psi_{Ex}(i,j) = 0, \text{ and} \quad (25)$$

$$f_2(i,j) + \psi_{Ey}(i,j) = -\psi_{sy}(i) + \psi_{oy}(j) + \psi_{Ey}(i,j) = 0, \quad (26)$$

It is important to note that Equations 25 and 26 are expressed by two types of look angle. The look angle (ψ_{Ox}, ψ_{Oy}) is provided by the auxiliary data, and is a function of image pixel j and lens distortion. The other look angle (ψ_{Sx}, ψ_{Sy}) is the angle between the predicted satellite position and the true ground position (see Figure 3). The look angle can be calculated by using ground position (p_x, p_y, p_z), satellite attitude, and the ephemeris point in terms of the image lines i. This look angle can be calculated by taking an arctangent to the left-hand side terms in Equations 18 and 19. Equations 25 and 26 expressed by these two look angles are functions of image lines and pixels, and consequently also are the error look angles functions of image lines i and pixels j. The $\psi_{Ex}(i,j)$ and $\psi_{Ey}(i,j)$ are functions of i and j depending on the difference between the true and predicted position and the difference between the true and predicted attitude of the sensor array, respectively. The differences are commonly modeled as a two-dimensional linear function of (i,j).

Let the additional correction term (ψ_{Ex}, ψ_{Ey}) for exterior orientation be line functions given by:

$$F_1 = kf_1 + k\psi_{Ex} = kf_1 + a_0 + b_0 \cdot i + c_0 \cdot j = 0, \text{ and} \quad (27)$$

$$F_2 = kf_2 + k\psi_{Ey} = kf_2 + a_1 + b_1 \cdot i + c_1 \cdot j = 0, \quad (28)$$

where a_0, a_1, b_0, b_1, c_0, and c_1 are the model parameters evaluated by adjusting the LOS vector, and k is a scaling parameter that is defined by the distance between the ground and the satellite position. This scaling parameter can approximately convert to the positional error on the ground from error look angle, and be calculated from the satellite height and the central look angle.

Using the method of bias-compensated Rational Polynomial Coefficients (RPC) bundle adjustment for Ikonos and QuickBird images (Fraser *et al.*, 2002; Noguchi and Fraser, 2004), the basic model for the LOS vector adjustment model is finally given by:

$$\begin{bmatrix} V_1 \\ V_2 \end{bmatrix}_{mn} = \begin{bmatrix} \frac{\partial F_1}{\partial p_x} & \frac{\partial F_1}{\partial p_y} & \frac{\partial F_1}{\partial p_z} & 1 & i & j & 0 & 0 & 0 \\ \frac{\partial F_2}{\partial p_x} & \frac{\partial F_2}{\partial p_y} & \frac{\partial F_2}{\partial p_z} & 0 & 0 & 0 & 1 & i & j \end{bmatrix}_{mn}$$

$$\times \begin{bmatrix} \delta p_{x_n} \\ \delta p_{y_n} \\ \delta p_{Z_n} \\ a_{0_m} \\ b_{0_m} \\ c_{0_m} \\ a_{1_m} \\ b_{1_m} \\ c_{1_m} \end{bmatrix} + k_m \begin{bmatrix} f_1 \\ f_2 \end{bmatrix}_{mn}, \quad (29)$$

where ν_1 and ν_2 are residuals, δp_x, δp_y and δp_z are corrections to approximates for the position vector $(\overrightarrow{p})$.

Although Equation 29 is formulated for one given point n on a single image m, it is possible to extend the model to an arbitrary number of points (either GCPs or tie points) on two or more images. The model parameters of the LOS vector are determined using Equation 29; thereafter geopositioning of the satellite image may be carried out by using Equations 27 and 28.

Whereas other methods use predicted orbit constraints as initial values to update orbit parameters, this proposed method exploits the LOS vector as well as the predicted parameters for accurate geopositioning of the distorted image without updating the orbit parameters. As there are six unknown model parameters (a_0, a_1, b_0, b_1, c_0, c_1) and two equations, the LOS vector adjustment model requires a minimum of three GCPs to solve Equations 27 and 28. The rationale of the proposed method is to avoid updating orbit parameters, as this often introduces additional errors. Because the predicted orbit information is relatively precise, it is possible to effectively achieve geometric correction of an image by adjusting the LOS vector with only a few GCPs.

Stereo Model Accuracy

Test Images

The potential accuracy of a SPOT-5 stereopair was evaluated using the LOS vector adjustment model. The tested stereopair consisted of a right image with 5.4° to 9.5° look angles and a left image with −26.0° to −21.9° look angles. This stereo pair was acquired on 07 April 2004 and 25 May 2004 in the Korean peninsular. The parameters from the SPOT-5 auxiliary data were used in the first step processing of the model. These auxiliary data included the corrected attitude angles, ephemeris points, look angles, and other information.

With the stable oscillator DORIS, SPOT-5 provides precise on-board time and ephemeris points every 30 seconds. In previous SPOT systems, the look angle at a given pixel was estimated using a simple linear function linking the first to the last detector. The linear relationship of look angles between detectors is not always determinable because of lens distortion. The look angles of SPOT-5 HRG are given for each detector as nonlinear values (Bouillon *et al.*, 2003). SPOT-5 also provides corrected attitude angles instead of the values of roll, pitch, and yaw angular speed. In the LOS vector adjustment model for SPOT-5 imagery, the look angles for each detector were used to correct the lens distortion. Five ephemeris points around the scene center time were used to calculate the LO–ECI rotation matrix M_E in Equation 6, and the AM–LO rotation matrix M_A was calculated from the corrected attitude angles.

Fifty points consisting of 12 GCPs and 38 checks of validity were selected in the image. They had a wide range of elevation, from 50 m to 1,290 m, and a scattered spatial distribution as seen in Figure 4. Geographic coordinates of the GCPs and check points were obtained from field survey, and the their accuracies are approximately 5 cm and 10 cm in planimetry and height, respectively

The Applicability of LOS Vector Adjustment Model

As shown by Equations 27 and 28, the residuals f_1 and f_2 of Equations 27 and 28 can be removed by the additional correction factors a_0, b_0, c_0, a_1, b_1, and c_1 in Equations 27 and 28, which are unknown parameters of the first-order polynomial transform. It is first necessary to show that the residuals are approximately a linear function of image lines i and pixels j. Figure 5 shows two-dimensionally scaled residuals of kf_1 and kf_2. These data are obtained by a natural neighbor interpolation using the 50 points. Figures 5a and 5b show the results from the right image of the stereo pair, and Figures 5c and 5d present the results of the left image. The scaled residuals kf_1 and kf_2 show positional errors on the ground because the parameter k is the distance between the ground and the satellite position, and residuals f_1 and f_2 are in fact the angles between the predicted and corrected LOS vectors. If the residuals are not removed, positional errors in the left image range from 118 m to 143 m, and those in the right image vary from 153 m to 167 m as shown by Figure 5. These errors correspond to about 47 to 67 pixels in the SPOT-5 image where the ground resolution is 2.5 m.

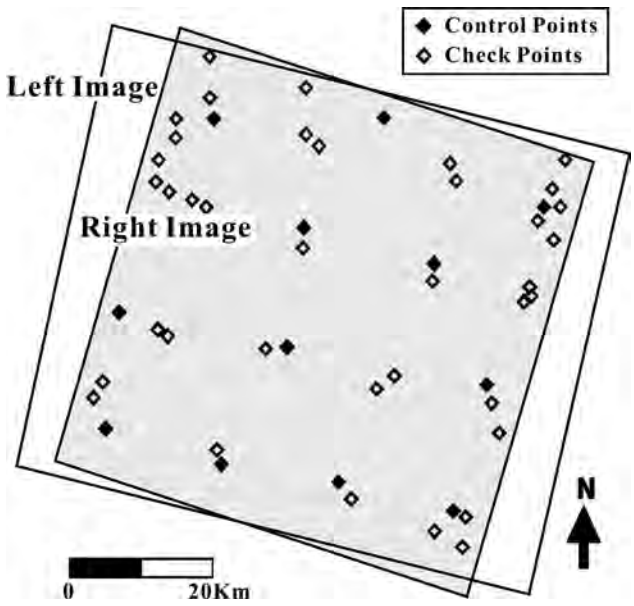

Figure 4. Distribution of 12 GCPs and 38 checkpoints. Open diamonds denote GCPs, and solid diamonds denote checkpoints.

The errors show relatively simple trends of systematic change with respect to image lines and pixels. The contour lines in Figure 5a indicate that the scaled residual kf_1 of the right image increases as lines or pixels increase. The changing pattern of the scaled residual kf_2 in Figure 5b also shows a similarity to Figure 5a except in the upper right of the image. The disturbance was caused by a 0.5 m error at a GCP. The linear property of the scaled residual kf_2 in the right image is thus preserved.

The contour lines in Figure 5c are not linear but slightly curved. The difference between the shape of the predicted orbit and that of the true orbit or errors of attitude angle account for the nonlinearity. As the contour lines are only slightly curved, we assume that the scaled residual kf_1 of the left image is a simple linear function of lines and pixels interacting in the positional accuracy. The scaled residual kf_2 of the left image (Figure 5d) is similar to that of Figure 5b. Figure 6 shows the coefficient of determination (R^2) and root mean square errors (RMSE) along profiles in Figures 5a and 5c. In profiles AA′ and BB′ (right image), the interpolated data are well fitted by a linear function with an R^2 of 0.99. The profile of CC′ (Figure 6c) is also well fitted to a line. The profile of DD′ is slightly curved with a relatively low R^2 of 0.93. Although the R^2 of the profile DD′ was the worst fit among the profiles, the RMSE was only about 0.2 m. These results lead us to make a simple approximation that the residuals of the SPOT-5 image are a two-dimensionally first-order function of lines i and pixels j.

Table 1 shows the result corrected by a first-order polynomial transform by using the 50 points. This result was obtained by adjusting the LOS vector of the right image by about −140 and −52.4 μrad in X and Y, respectively, and of the left image by about −157 and −69.8 μrad in X and Y, respectively. The RMSEs were of 0.60 m and 0.12 m for kf_1 and kf_2 for the right image, respectively, and of 0.99 m and

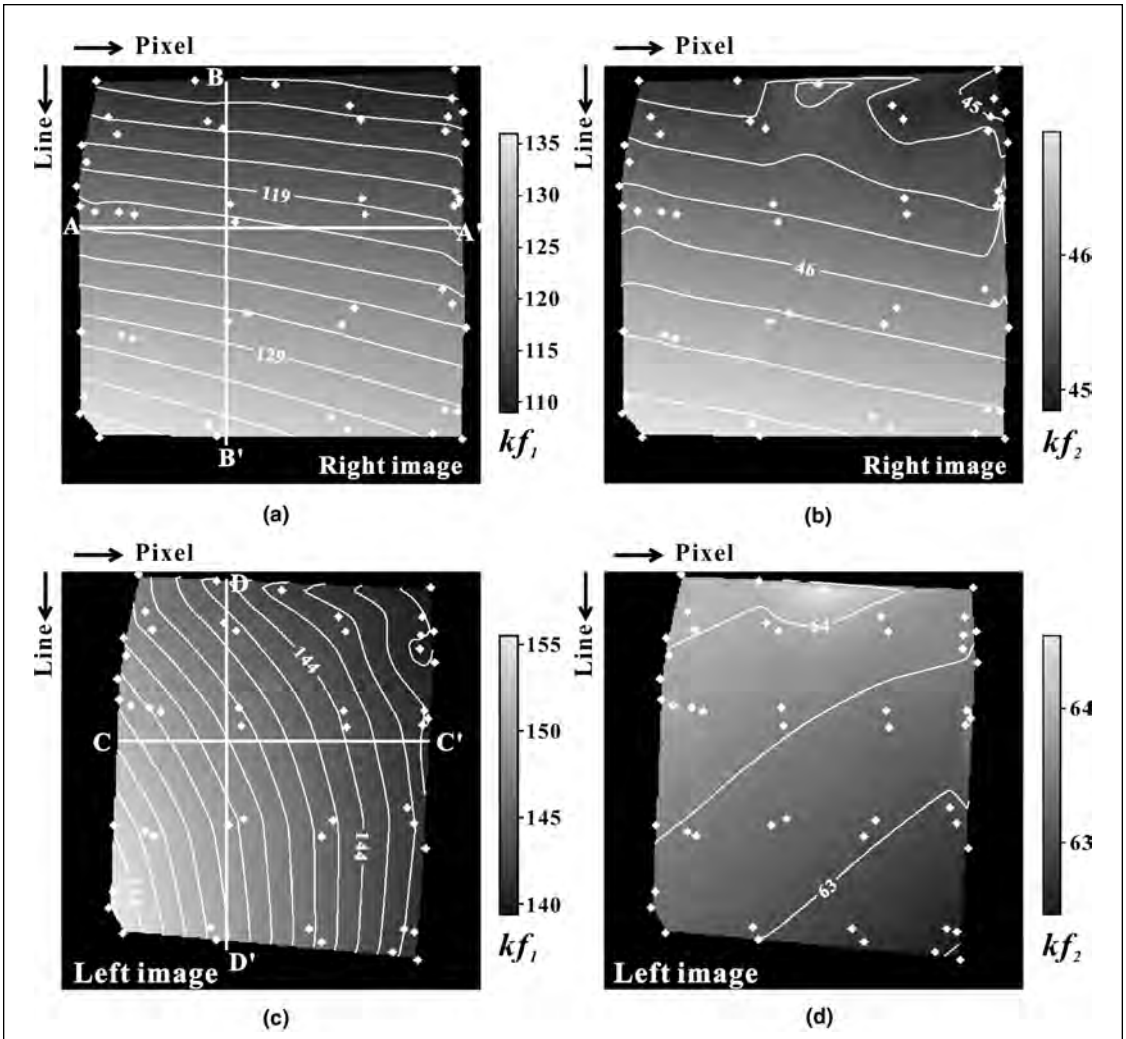

Figure 5. Two-dimensional scaled residuals kf_1 and kf_2 in the tested SPOT-5 stereo pair. (a) kf_1 of right image, (b) kf_2 of right image, (c) kf_1 of left image, and (d) kf_2 of left image.

0.12 m for kf_1 and kf_2 in the left image, respectively. Residuals can therefore be significantly eliminated by a first-order polynomial transform.

Spatial Distribution of GCPs

The minimum required number of GCPs for a LOS vector adjustment model is three. However, if three-dimensional geopositioning of a SPOT stereo pair is determined by using only three GCPs, their spatial distribution is very important. We tested the accuracy with respect to the distribution of GCPs using six groups as shown in Figure 7. Groups 1 through 3 in Figure 7 consist of three GCPs in a triangle, and groups 4 through 6 are characterized by GCPs along a straight line. Table 2 shows the minimum and maximum errors of checkpoints in X, Y, and Z, and the RMSEs in planimetry and height for six groups. In Table 2, groups 4 through 6 show substantially less accuracy compared with groups 1 through 3, as would be expected. The accuracy within groups 1 through 3 is at least three times higher than that within groups 4 through 6. Group 5 in particular gave the least accuracy because the residuals f_1 and f_2 in Equations 27 and 28 largely depend on pixel number j rather than line number i. The test results indicate that the distribution of GCPs significantly affects the accuracy of three-dimensional geopositioning, and that GCPs must be widespread throughout the image in common with other methods.

Number of GCPs

We have tested the accuracy of the LOS vector adjustment model with respect to the number of GCPs used. Three to 12 GCPs were taken for the geometric correction, and 38 checkpoints were selected to evaluate the accuracy of each case. The RMSEs of GCPs and checkpoints corresponding to the number of GCPs are summarized in Table 3 and Figure 8. Table 3 shows the minimum and maximum values of the errors and RMSEs of 38 checkpoints when three, five, and 12 GCPs were used. In the illustrations, the RMSEs of checkpoints rapidly decreases when the number GCPs increases up to five. With more than five GCPs, there is relative stability (Figure 8a). The RMSEs of GCPs also shows similar trends, rapidly increasing up to five GCPs and a near constant value from five to 12 GCPs.

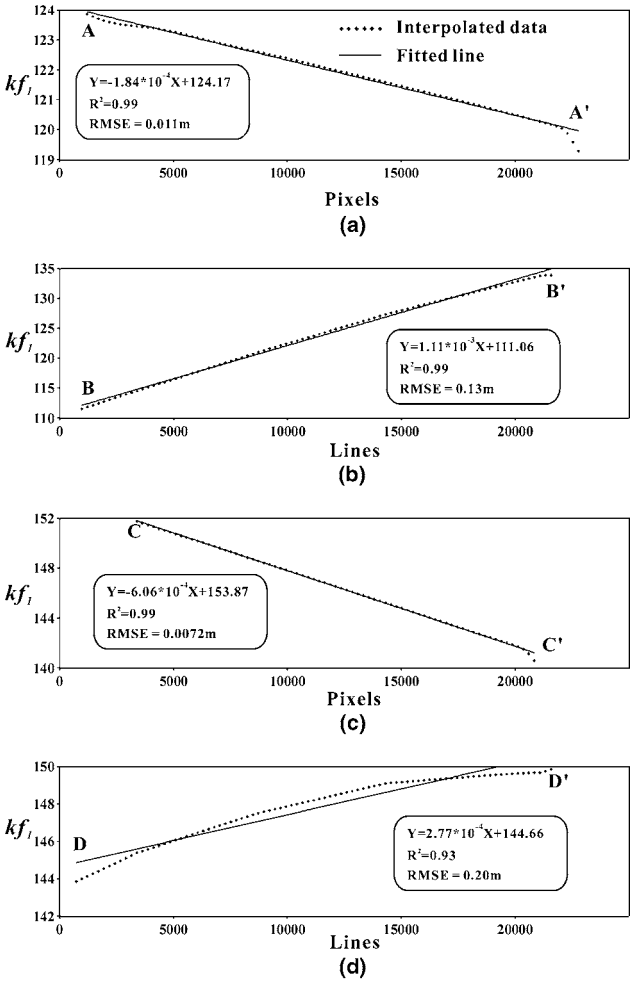

Figure 6. Evaluation of linear model by using coefficient of determination (R^2) and RMSEs along profiles. (A) through (D) respectively display the profiles of AA′ through DD′ in Figure 5a and 5c.

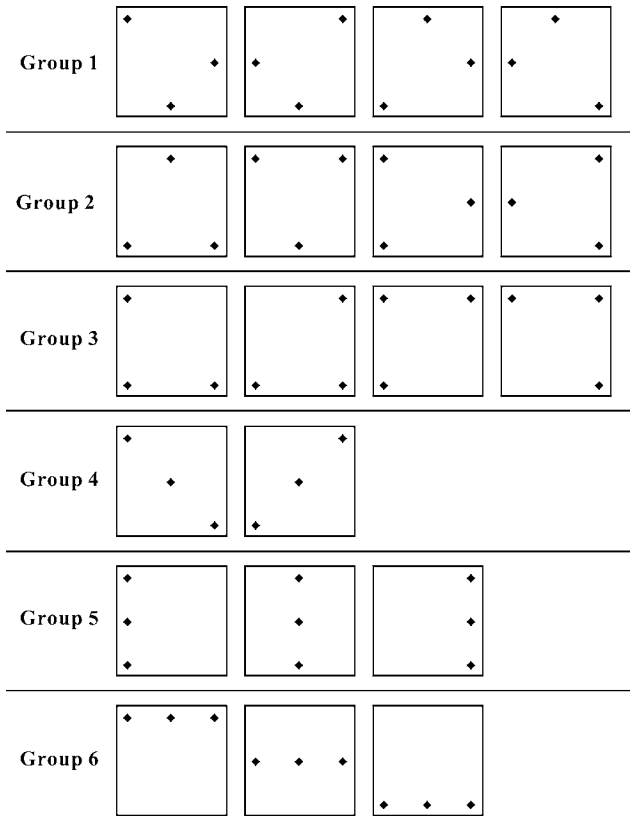

Figure 7. Six groups of GCPs for testing the effect of GCP distribution.

TABLE 1. ERROR STATISTICS OF THE SCALED FUNCTIONAL RESIDUALS THAT ARE CORRECTED BY A FIRST-ORDER POLYNOMIAL TRANSFORM

Image	Error of kf_1 (m)			Error of kf_2 (m)		
	Min.	Max.	RMSE	Min.	Max.	RMSE
Right	–1.43	0.79	0.60	–0.16	0.59	0.12
Left	–2.40	1.43	0.99	–0.23	0.61	0.12

These results imply that the RMSEs of GCPs and checkpoints become stable with five properly distributed GCPs. In the practical application of the LOS vector adjustment model, one needs at least five well-distributed GCPs. The RMSE in the Z direction is higher than the RMSEs along the X and Y directions. Using only three well-distributed GCPs, the LOS vector adjustment model resulted in RMSEs of 0.79 m and 1.08 m in planimetry and height, respectively. The performance of the LOC vector adjustment model thus satisfies the RMSE within one pixel of SPOT-5 even when only three GCPs are selected. The RMSEs were further improved to 0.48 m and 0.64 m in planimetry and height, respectively, when five GCPs were involved. Improvement of the RMSEs using six or more GCPs was not significant. The performance of the LOS vector adjustment model was compared with that of bundle adjustment.

TABLE 2. ACCURACY OF CHECKPOINTS FOR SIX GROUPS WHEN THREE GCPS WERE USED

Group No.	X error (m)		Y error (m)		Z error (m)		RMSE (m)	
	Min.	Max.	Min.	Max.	Min.	Max.	Plan.	Height
1	–0.41	0.76	–2.38	1.82	–1.88	2.91	0.94	1.03
2	–0.41	0.73	–1.85	1.58	–1.87	3.06	0.77	1.02
3	–0.62	0.34	–2.12	1.84	–3.16	3.75	0.81	1.33
4	–5.22	4.69	–6.30	5.66	–7.53	9.13	3.34	3.96
5	–3.44	15.10	–47.87	21.37	–12.72	49.37	20.85	18.80
6	–3.81	1.96	–5.98	1.23	–3.44	8.27	2.30	2.81

TABLE 3. ACCURACY OF CHECKPOINTS AFTER GEOMETRIC CORRECTION BY USING THREE, FIVE, AND 12 GCPS

No. of GCPs	X error (m)		Y error (m)		Z error (m)		RMSE (m)	
	Min.	Max.	Min.	Max.	Min.	Max.	Plan.	Height
3	–0.41	0.50	–1.83	0.52	–0.40	2.68	0.79	1.08
5	–0.48	0.25	–0.90	0.63	–0.87	1.27	0.48	0.64
12	–0.24	0.46	–0.98	0.54	–0.73	1.39	0.46	0.66

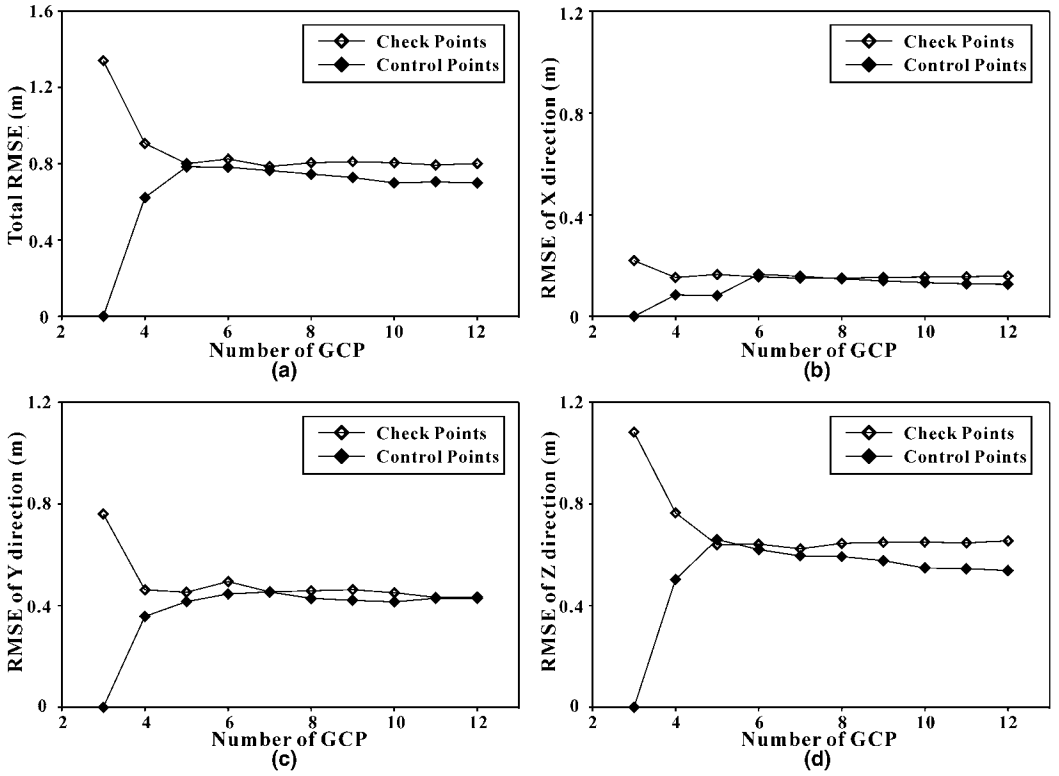

Figure 8. RMSEs of GCPs and checkpoints according to the number of GCPs. (a) Total RMSE, (b) RMSE in X, (c) RMSE in Y, and (d) RMSE in Z. Note that RMSEs become stable by using five or more GCPs.

Bundle adjustment was applied using the commercial package ERDAS 8.7 Leica Photogrammetry Suite (LPS) module. Second order polynomials were used for the model parameters of satellite positions and the yaw angle, and the effect of the Earth curvature was also considered. Twelve GCPs were used for the bundle adjustment model, and errors at 36 checkpoints were analyzed. Figure 9 gives the comparison between the LOS vector adjustment and the bundle adjustment models with 12 GCPs. The RMSEs of the bundle adjustment model were 2.21 m and 1.34 m in the planimetry and height, respectively. The RMSEs of the LOS vector adjustment model using 12 GCPs were 0.15 m, 0.43 m, and 0.66 m in the X, Y, and Z directions, respectively. The accuracy using LOS vector adjustment might be better than that of bundle adjustment. The accuracy in the X direction particularly was high, as seen in Figure 9a. On the basis of the results obtained with ERDAS 8.7 LPS bundle adjustment software, it would appear that the proposed method can produce superior results to the bundle adjustment model, as seen in Figure 9 and the estimated RMSEs. This result demonstrates that the LOS vector adjustment method can be efficient in geopositioning of SPOT-5 HRG image using fewer GCPs.

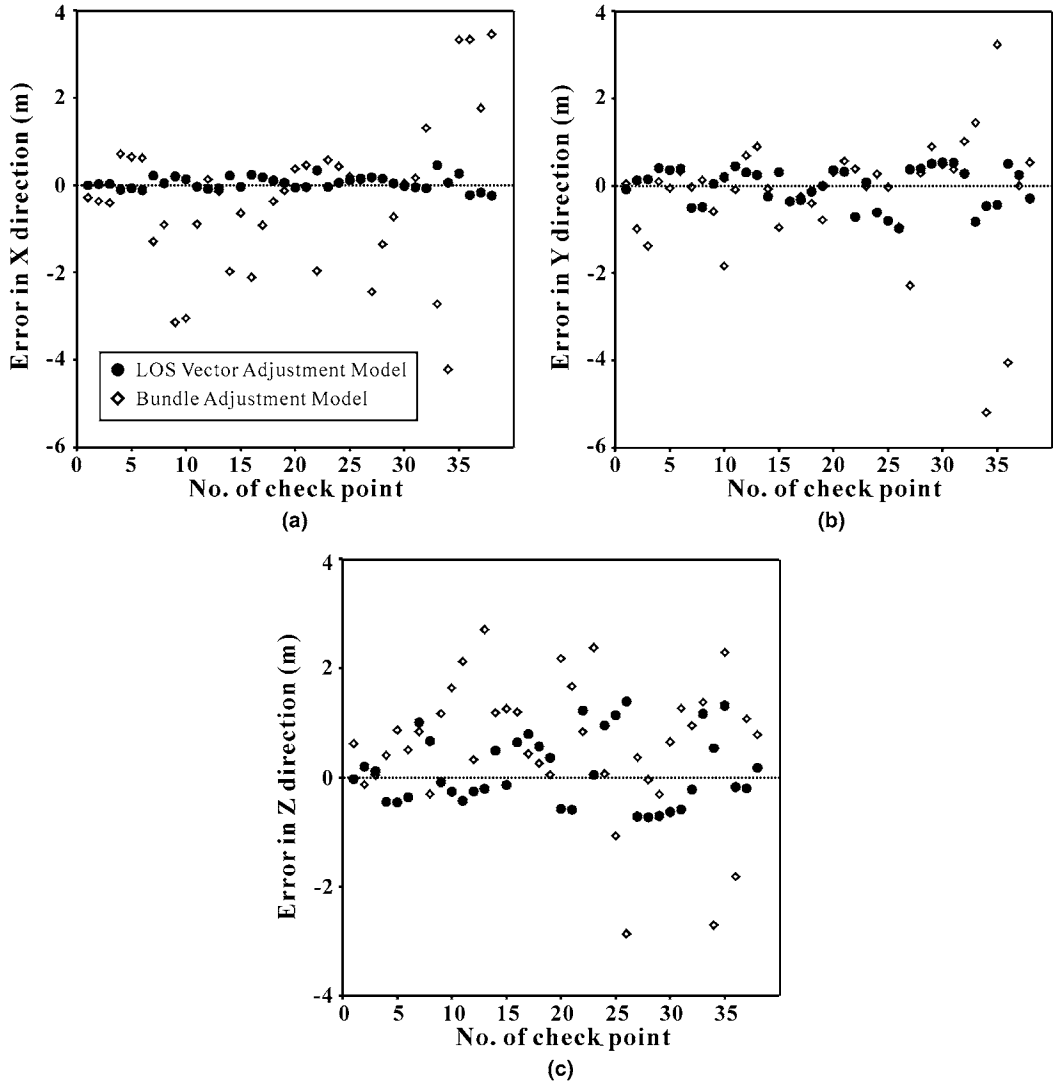

Figure 9. The comparison between the LOS vector adjustment model and the bundle adjustment model using 12 GCPs. (a), (b), and (c) represent errors of checkpoints of the two models in the X, Y, and Z direction, respectively.

Conclusions

The LOS vector adjustment model was formulated from satellite geometry for the geopositioning of SPOT-5 images. The core idea of the method is to adjust the LOS vector only when correcting from the predicted ground position to the true position. The LOS vector adjustment model was derived with two assumptions: (a) that the satellite is moving along a well-defined close-to-circular elliptical orbit; and (b) that the predicted orbit recorded in auxiliary data is close to the true satellite orbit. The SPOT-5 system satisfies both assumptions. An advantage of the proposed method is that accurate geopositioning can be achieved even with a limited number of GCPs. The performance of the method was tested using a SPOT-5 stereo pair. The distribution of GCPs was important in achieving accurate geopositioning. A triangular distribution of three GCPs produced the best result. Even with only three GCPs, the test satisfactorily achieved geopositioning accuracy within one pixel of the SPOT-5 image. The performance of the method with a variable number of GCPs was also tested. The RMSE of the checkpoints decreased up to five GCPs, and was stable from five to 12 GCPs. This result implies that five GCPs is the optimal number in the practical application of the LOS vector adjustment model. With five GCPs, the RMSEs were 0.48 m and 0.64 m in planimetry and height, respectively. The proposed LOS vector adjustment model performed better than the bundle adjustment model in all respects, and is an effective method for the geopositioning of SPOT-5 stereopairs.

References

Baraldi, A., and F. Parmiggiani, 1990. Urban area classification by multispectral SPOT images, *IEEE Transactions on Geoscience and Remote Sensing*, 28(4):674–680.

Bouillon, A., E. Breton, F. De Lussy, and R. Gachet, 2003. SPOT-5 geometric image quality, *Proceedings of IGARSS 2003*, 21–25 July, Toulouse, France, pp. 303–305.

Buyuksalih G., G. Kocak, H. Topan, M. Oruc, and A. Marangoz, 2005. SPOT revisited: Accuracy assessment, DEM generation and validation from stereo SPOT 5 HRG images, *The Photogrammetric Record*, 20(110):130–146.

Chen, L.C., and J.Y. Rau, 1993. A unified solution for digital terrain model and orthoimage generation from SPOT stereopairs, *IEEE Transactions on Geoscience and Remote Sensing*, 31(6):1243–1252.

Fraser, C.S., H.B. Hanley, and T. Yamakawa, 2002. Three-dimensional geopositioning accuracy of IKONOS imagery, *The Photogrammetric Record*, 17(99):465–479.

Gugan, D.J., and I.J. Dowman, 1988. Topographic mapping from SPOT imagery, *Photogrammetric Engineering & Remote Sensing*, 54(10):1409–1414.

Gupta, R., and R.I. Hartley, 1997. Linear pushbroom camera, *IEEE Transactions on Pattern Analysis and Machine Intelligence*, 19(9):963–975.

Jung, H.-S., S.-W. Kim, and J.-S. Won, 2004. The simple method of geometric reconstruction for SPOT images, *Proceedings of International Symposium on Remote Sensing*, 27–29 October, Jeju, Korea, pp. 205–207.

Kratky, V., 1989. Rigorous photogrammetric processing of SPOT images at CCM Canada, *ISPRS Journal of Photogrammetry and Remote Sensing*, 44:53–71.

Mahapatra, A., R. Ramchandran, and R. Krishnan, 2004. Modeling the uncertainty in orientation of IRS-1C/1D with a rigorous photogrammetric model, *Photogrammetric Engineering & Remote Sensing*, 70(8):939–946.

Noguchi, M., and C.S. Fraser, 2004. Accuracy assessment of QuickBird stereo imagery, *The Photogrammetric Record*, 19:128–137.

Nonin, P., and S. Piccard, 2003. Performance analysis of DEM automatic extraction from SPOT-5 sensors, *Proceedings of IGARSS 2003*, 21–25 July, Toulouse, France, pp. 309–311.

Orun, A.B., and K. Natarajan, 1994. A bundle adjustment software for SPOT imagery and photography: Tradeoff, *Photogrammetric Engineering & Remote Sensing*, 60(12):1431–1437.

Radhadevi, P.V., T.P. Sasikumar, and R. Ramachandran, 1994. Orbit attitude modeling and derivation of ground co-ordinates from spot stereopairs, *ISPRS Journal of Photogrammetry and Remote Sensing*, 49(4):22–28.

Radhadevi, P.V., R. Ramachandran, and A.S.R.K.V. Murali Mohan, 1998. Restitution of IRS-1C PAN data using an orbit attitude model and minimum control, *ISPRS Journal of Photogrammetry and Remote Sensing*, 53(5):262–271.

Salamonowicz, P.H., 1986. Satellite orientation and position for geometric correction of scanner imagery, *Photogrammetric Engineering & Remote Sensing*, 52(4):491–499.

Slama, C.C., C. Theurer, and S.W. Henriksen, 1980. *Manual of Photogrammetry*, Fourth edition, American Society of Photogrammetry.

Westin, T., 1990. Precision rectification of SPOT imagery, *Photogrammetric Engineering & Remote Sensing*, 56(2):247–253.

Yesou, H., and J. Rolet, 1990. Regional mapping of the South Armorican shear zone (Brittany, France) using remotely sensed SPOT imagery, *ISPRS Journal Photogrammetry and Remote Sensing*, 45:419–427.

Zoej, M.J.V., and G. Petrie, 1998. Mathematical modeling and accuracy testing of SPOT Level 1B stereopairs, *The Photogrammetric Record*, 16:67–82.

(Received 15 November 2005; accepted 30 January 2006; revised 18 April 2006)